Setup for Precise Measurements of beta-decay in Optically Trapped Radioactive Na

Sohani, Moslem

Chapter 4

TRIμP - Overview, Recent Improvements and New Components

Probing the SM and its proposed extensions at low energies requires high precision experiments at the limits of present technology. Precision measurements on nuclear β-decay need a detection system for low and intermediate energy charged particles that can resolve as many as possible observables and also deliver sufficient statistics. The TRIμP facility is developed to conduct such high precision studies [Jun02, Jun03, Wil05, Wil02]. In this chapter, an overview of the TRIμP facility is presented. The recent developments concerning low energy beam transport and optical trapping, which were performed in the framework of this work, are discussed. The principle of a precision β-decay measurement is explained and the new mechanical and optical details specific for a first β-decay experiment on ^{21}Na are described.

4.1 TRIμP Facility

The TRIμP facility consists of a dual magnetic separator after a gas target at typically atmospheric pressure as the isotope production stage. Several cooling and trapping stages reduce the energy of the radioactive particles from GeV down to neV. Cold radioactive atoms are trapped in an atom trap at the center of the β-decay detection system. The separator and cooling stages were designed and developed since 2001 [Ber06a, Tra06]. The properties of these parts and the achievements with them are discussed in this section.

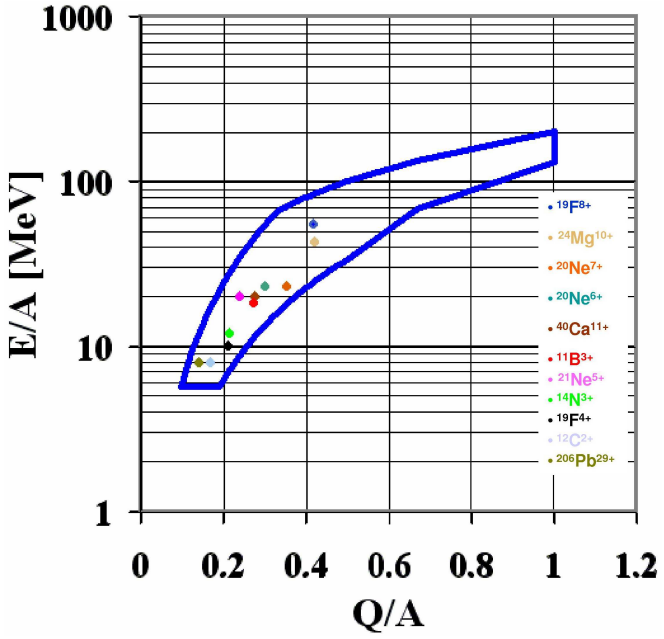

Fig. 4.1: Operating diagram (energy versus charge-mass ratio) for AGOR. The circles represent the beams which have been prepared for TRIμP experiments up to now [Hof08].

4.1.1 Separator

The superconducting AGOR cyclotron [Bra01, Bei05, Kre05] at KVI produces the primary beam for the TRIμP facility (see Fig. 4.1). Heavy ion beams up to 100 MeV/nucleon have been produced with powers up to 300 W. An upgrade program towards a 1 kW ion beam has been started.

In the production stage secondary beams of radioisotopes are produced with sufficient intensity in order to fulfill the statistics requirements of the precision experiments. Mostly direct, fragmentation or fusion-evaporation reactions are used in inverse kinematics [Ber06a, Ber06b, Tra07]. An overview of the separator is given in figure 4.2. A liquid nitrogen cooled gas target or a solid target ladder can be used. Secondary particles are passed through the first part of the separator and are dispersed at the intermediate focal plane according to their momentum. At this position the unwanted part of the momentum spectrum can be cut out using a pair of beam scrapers. The remaining beam, which consists of the isotope of interest and other particles with the same magnetic rigidity, passes through a thin piece of material, typically an Al foil. This material causes a mostly Z-dependent energy and momentum difference. Therefore, the second part of

the double separator can separate the contaminant nuclides from the isotope of interest. The purity of the secondary radioactive beam at the end of the separator depends on many parameters, e.g. the energy spread of the secondary beam and the type of the production reaction [Tra07]. This aspect is discussed extensively in [Tra06] and [Rog07].

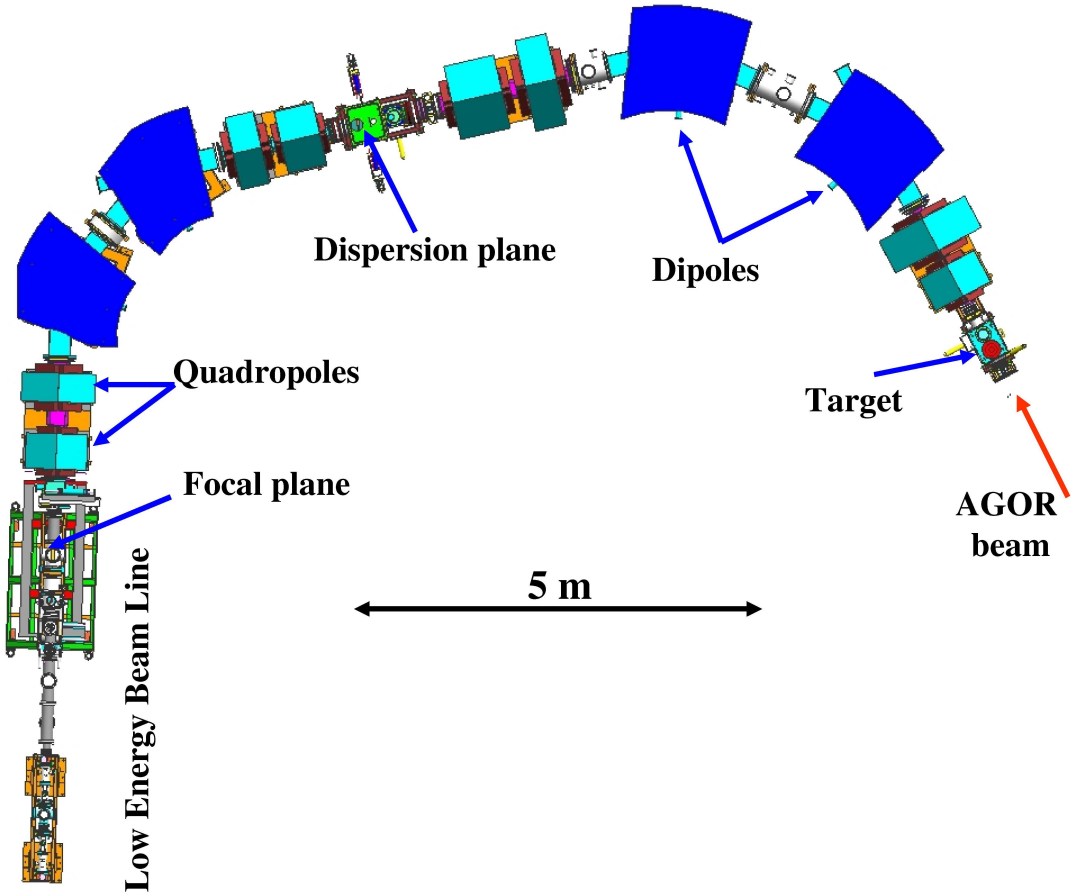

Fig. 4.2: Layout of the TRIμP production target, separator and low energy beam line.

Typical production rates achieved up to now are 10^4 particles per second and per nA primary beam (corresponding to a power of 0.46 W at 23 MeV beam) for ^{21}Na, ^{20}Na or ^{19}Ne. For example, a measurement of the β-decay branching ratio in ^{21}Na decay could be performed using the clean secondary beam at TRIμP [Ach05]. The D_2 gas target which has 10 cm length has been operated at pressures up to 5 bar in order to increase the target thickness and therefore the production rate, which rises linearly with the target pressure.

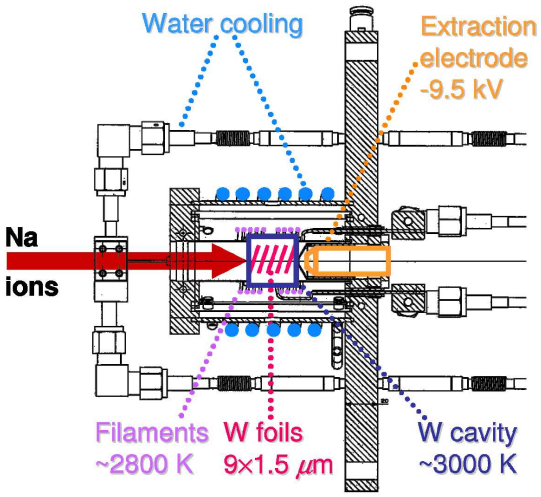

Fig. 4.3: Layout of the TRIμP thermal ionizer.

4.1.2 Low Energy Radioactive Beam

In order to perform the envisaged precision measurements, radioactive ions need to be cooled, neutralized and trapped in atom traps. The cooling procedure needs to be fast and efficient in view of the short lifetime of the isotopes, which are of particular interest, e.g. ^{20}Na,^{21}Na,^{19}Ne,^{39}Ca and ^{213}Ra. For light isotopes such as ^{21}Na, the high energy and fully stripped secondary beam passes through several cooling stages. Then it can be delivered as a low energy and singly charged ion beam with acceptable emittance.

The first cooling stage after the separator is a thermal ionizer (TI). The TI is a device which consists of several tungsten (W) foils to stop the beam. The foil stack is housed in a W cavity (see Fig. 4.3). Neutral atoms defuse out of these foils at high temperature. Collisions with the surface of the foils and the cavity body can ionize these atoms with a probability [Lan25]

$$\alpha_s \propto \exp\left(\frac{\phi - W_i}{kT}\right), \tag{4.1}$$

where T is the temperature of the foil, ϕ and W_i are the work function of the metal and the first ionization potential of the atoms. An electric field allows to extract ions through a small (2 mm diameter) exit hole. For the TI the choice of the material is critical. It is important that the isotopes of interest should have a high diffusion constant inside the stopper material, which depends on the material of the stopper foils and their temperature. Further, a high work function of the material favors surface ionization. The difference between the ionization

potential of the beam particles and the foil material determines the ionization probability and re-neutralization after each collision with a surface. Therefore a TI mainly works for alkali and alkali-earth elements that have low ionization potentials [Kir90]. For alkali metals W at a temperature $T \simeq 2800$ K appears to be the right choice for stopping foils. For ^{21}Na an extraction efficiency of 50% was achieved [Tra06]. For ^{20}Na this was 18% due to the isotope's shorter lifetime (see Tab. 3.1).

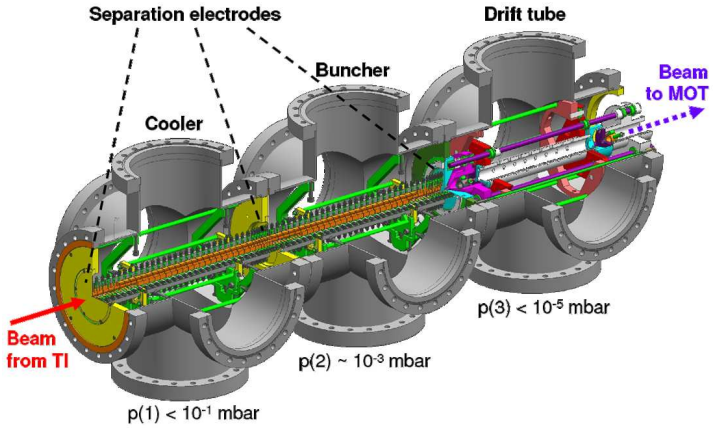

Fig. 4.4: The Radio Frequency Quadrupole (RFQ) as a cooler and buncher.

Ions extracted from TI pass through a Wien-filter for mass selection (see Fig. 4.5). It is a region of crossed electric and magnetic field ($E \times B$) orthogonal each on the beam axis. Our device has electrodes of $l_E = 92$ cm length and uses an effective magnetic field of $B = 200$ mT over a length of $l_B = 80$ cm. Ions of mass m and energy ε can pass the filter undeflected, for an electric field of

$$E = \sqrt{\frac{2\varepsilon}{m}} B. \tag{4.2}$$

The Wien-filter therefore provides mass selection. It was designed here to achieve a resolution of one mass unite in the region of Na isotopes. After the Wien-filter the ions can be coupled into a gas filled two stage radio frequency quadrupole (RFQ) which acts as a cooler and buncher (see Fig. 4.4). The device has two stages with 10^{-2} and 10^{-3} mbar He pressure and a radio frequency (Paul) trap at the end to accumulate ions. The transverse energy of the ions is cooled in collisions with helium atoms in the first section of the system. The ions are radially confined with an RF field and drift to the second part. The ions are collected at the end of the buncher section in an RF ion trap. This trap can be switched to give bunched pulses. A bunch of ions can be extracted towards

an atom trap through a pulsed drift tube and a set of electrostatic ion optics elements (two Einzel lenses and two pairs of steering capacitors), which form the low energy beam line (LEB). Typical ion energies are between 3 and 10 keV. Details of the design and properties of the RFQ system are given in [Tra06]. Recent measurements show that the RFQ and the LEB system have a total transmission of about 40% for ^{21}Na. Table 4.1 displays the efficiencies of the RFQ parts measured with a stable ^{23}Na ion source. If slow bunching is not required the RFQ can be replaced by a pulsed drift tube, which has a measured maximum transmission of 50%. It is a 1 m long metal tube of 4 cm inner diameter inside the vacuum system.

Table 4.1: Main RFQ cooler and buncher properties obtained from off-line measurements with a stable ^{23}Na (from [Tra06]-the uncertainties in the efficiencies have been estimated from the data given there for quantitative comparison in the future).

Cooler efficiency	56(6)%
Buncher efficiency (continuous mode)	58(6)%
Minimal trap capacity	$5 \cdot 10^4$ ions
Extraction time range	10^{-3} - 1 s

Thermal ionization and laser trapping are working for alkaline and alkaline earth elements very well. As discussed in section 2.1 there are several isotopes of interest for precision β-decay studies and EDM researches among these elements. Therefore the TI fits very well as an ion catcher in the TRIμP β-decay and EDM research programs. Other options such as a gas filled ion catcher can be added later for other elements [Mor06, Den06a, Den06b] in particular for nobel gases, if needed.

4.1.3 Atom Traps

The β-decay experiments at the TRIμP facility will be carried out using a set of two coupled magneto-optical traps. The first trap collects atoms from the radioactive beam (collector MOT) [Rog07]. From there they are moved to a second trap inside a detection chamber (measurement MOT).

The vacuum vessel for the first trap is made of glass. It has six 2.5 cm diameter windows to allow rather large diameter ($\approx$1 cm) laser beams for efficient atom

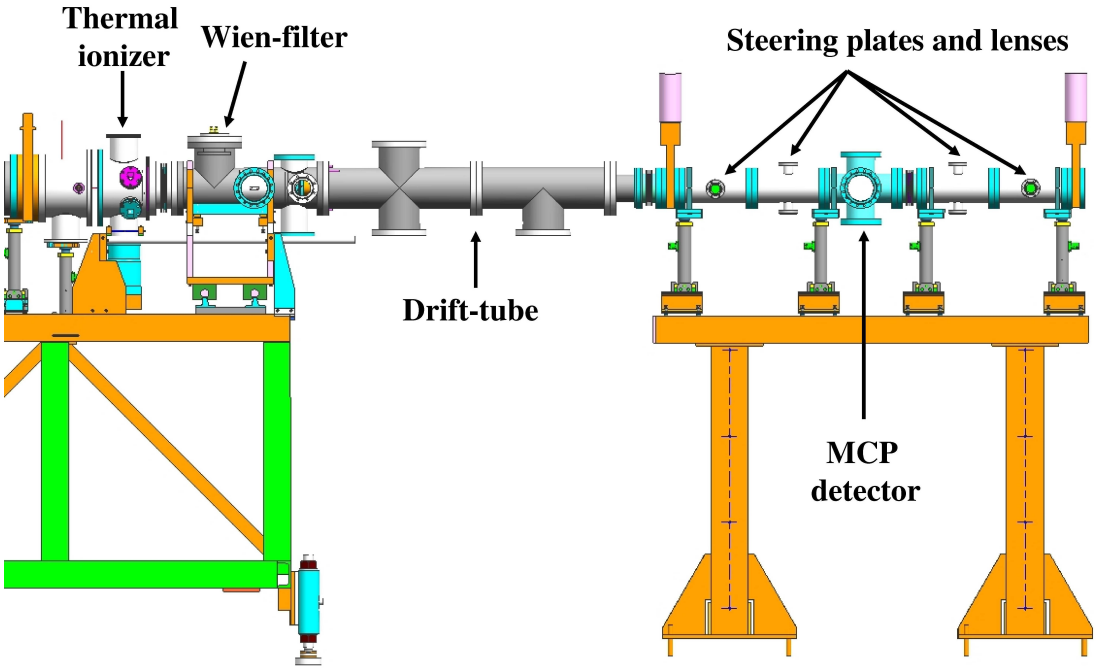

Fig. 4.5: Low energy beam line including the thermal ionizer, Wien-filter, drift-tube and ion optical elements is a transport line for low energy ions extracted from the thermal ionizer to the collector MOT cell. For part of the measurements the RFQ was replaced by the shown 1 m long drift tube.

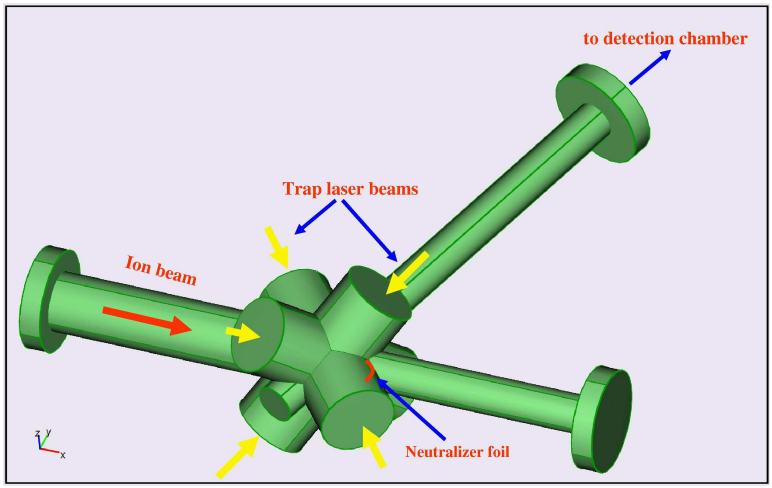

Fig. 4.6: Schematic view of the collector MOT cell.

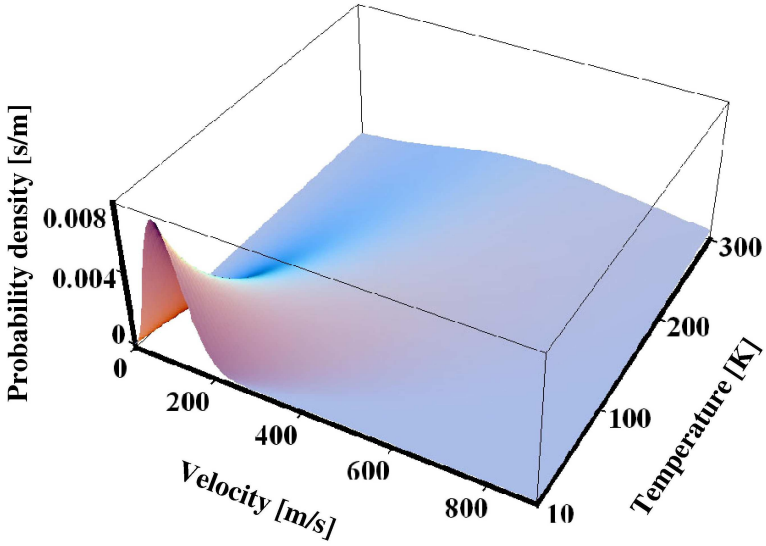

Fig. 4.7: Maxwell-Boltzmann velocity distribution of ^{23}Na atoms for temperatures (< 300°K).

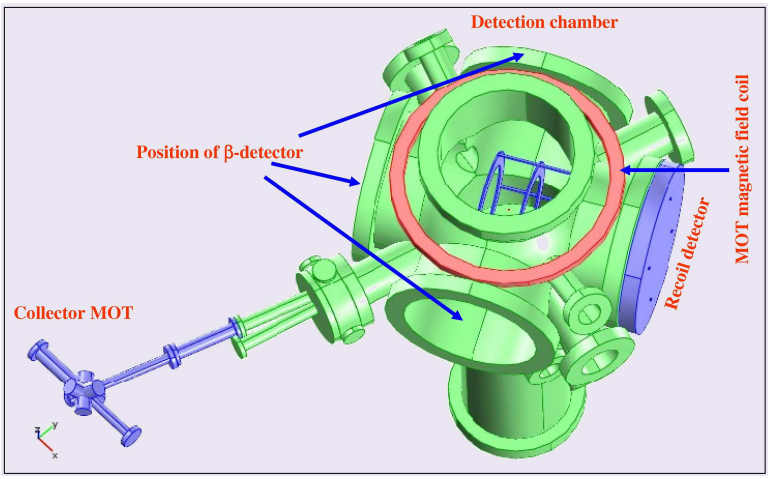

Fig. 4.8: Atomic trap and detection setup.

collection (see Fig. 4.6). It contains a hot zirconium foil to neutralize the incoming ion beam.

Atoms in a thermal gas have velocities according to the Maxwell-Boltzmann distribution (see Fig. 4.7). A small fraction of the atoms have velocities smaller than the typical capture velocities (see Fig. 3.9). In a closed chamber higher velocity atoms has a chance to redistribute over the velocities by collisions with the wall. A special dry-film wall coating (SC-77) in the glass cell minimizes the wall sticking time for the atoms [Fed97]. For the current geometry of the collector cell (see Fig. 4.6), the coating increases the number of bounces with the wall by a factor of about 5. A drawback of the coating is that the optical windows are also coated with this film, which causes straying of the laser light and it increases the laser light losses on every pass through the cell windows.

The second trap is located in a precision measurement chamber and centered in a reaction microscope and a β-detector (see Fig. 4.8 and 4.18). These two trap chambers are connected with a narrow pathway tube. A push beam and a catch beam will send and receive the cold atoms from the first to the second trap. Two transverse cooling stages are provided to prevent atoms to escape transversely from the atom bunch in between.

4.2 Recent Improvements of the LEBL

In this work we expand over the achievements of [Tra06] and [Rog07] concerning the optimization and understanding of the TI performance, the transport of the ions to the collector MOT, the neutralizer foil properties and the trapping efficiency.

4.2.1 Thermal Ionizer Performance

The TI performance was studied and improved using ^{21}Na ions from the TRIμP separator. They were transported from the TI to the neutralizer in the trap cell and they were counted by observing the 511 keV back-to-back γ-rays from positron annihilation coincidentally using two scintillator detectors mounted on opposite sides of the neutralizer foil. Experiments to measure the TI output were performed in two experimental modes. First, the accelerator beam was chopped in a cycle with t=125 seconds beam on and 125 seconds beam off, where t=125 s is much longer than the $T_{1/2}(^{21}\mathrm{Na})$=22.4 s half-life time of ^{21}Na. In the second mode, the extraction voltage of the TI was cycled with the same “on” and “off”

time periods. In the "on" phase of the experiment the 511 keV activity from the neutralizer increases to an equilibrium value. The activity decays during the beam off period. In the mode when the primary beam is always on, the output radioactive ion beam of the TI is constant. Switching the extraction "on" and "off" produces a loading and decay of the activity at the measuring site that depends only on the lifetime of the extracted isotope. If the extraction is left on and the primary beam is toggled "on" and "off", then the time which radioactive particles spend in the TI influences the time dependence of the 511 keV γ-ray rate (see Fig. 4.9). In the latter mode, the output is delayed and continues longer as compared to the first mode. We can model this effusion with the assumption that there is a mean time τ_{TI} which a particle stays in the TI. The emission from the TI is then

$$\frac{dS}{dt} = I - \lambda_e\, S - \lambda_d\, S - \lambda_x\, S = I - \lambda_S\, S, \tag{4.3}$$

where S is the number of particles in the TI, I is the rate of incoming particles into the TI, $\lambda_e = \tau_{TI}^{-1}$ is the rate corresponding to the extraction from the TI, λ_d is the decay rate of the radioactive isotope, λ_x is the loss rate due to other leaks in the TI. λ_S is the total particle loss in the TI. The observed time dependence of the TI activity can be described by

$$A_{Bon} = \frac{\lambda_e\, I}{\lambda_s}\{(\frac{1}{\lambda_d} - \frac{1}{\lambda_d - \lambda_s}\, e^{-\lambda_s t}) + (\frac{1}{\lambda_d - \lambda_s} - \frac{1}{\lambda_d})\, e^{-\lambda_d t}\}\lambda_d. \tag{4.4}$$

for the beam "on" period and

$$A_{Boff} = \frac{\lambda_e\, I}{\lambda_s}\{\frac{e^{-\lambda_s t}}{\lambda_d - \lambda_s} + (\frac{1}{\lambda_d} - \frac{1}{\lambda_d - \lambda_s})\, e^{-\lambda_d t}\}\lambda_d. \tag{4.5}$$

for the beam "off" period. Here $\lambda_s = \lambda_e + \lambda_d$. In the second mode, where the beam is always on, the TI extraction "on" and "off" phases give

$$A_{TIon} = \frac{\lambda_e\, I}{\lambda_s}(1 - e^{-\lambda_d t}) \quad \text{and} \quad A_{TIoff} = \frac{\lambda_e\, I}{\lambda_s} e^{-\lambda_d t}. \tag{4.6}$$

In this calculation the effect of the diffusion of Na atoms from the stopper foils inside of the TI is not explicitly included and the functioning of the TI is contracted in the extraction rate λ_e of the TI.

The half-life τ_{TI} of the ^{21}Na ions in the TI is extracted by fitting the activity curves to the observed 511 keV γ-ray rate in both modes of TI extraction and for beam "on" and "off" (see Fig. 4.9). The half-life $T_{TI}^{1/2}$ is shorter at higher temperatures, because of larger ionization probability and higher atomic velocity

(see Fig. 4.10). For $T_{TI}^{1/2} \ll T_{^{21}\mathrm{Na}}^{1/2}$, i.e. when the half-life of ions in the TI gets shorter than the radioactive half-life of ^{21}Na, the maximum rate of extracted particles from the TI saturates.

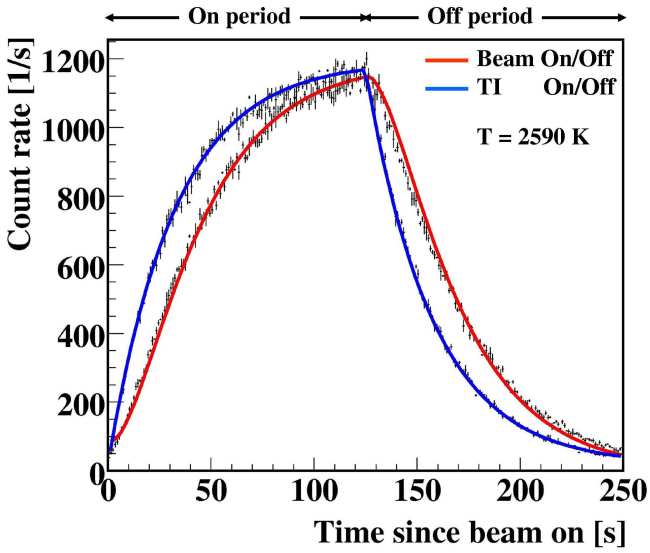

Fig. 4.9: Rate of the registered 511 keV γ-rays at the neutralizer position on one of the scintillator detectors. Fit results for cyclotron beam switching (solid curve) and TI extraction switching (dashed curve) are shown. The temperature of the TI is 2590(50) K as determined by a pyrometer. The half-life time of the TI is $T_{1/2}(TI)$ =20 s.

4.2.2 Pulsed Drift Tube

In the framework of this work a pulsed drift tube device was developed that can replace the RFQ for measurements of the Wien-filter performance and for experiments where the short pulsing capability of the RFQ is not relevant. A drift tube allows to connect the TI and the atomic traps, which both can be kept at ground potential. An accelerated beam of several keV can be transported (see Fig. 4.5). The drift tube is operated at the voltage potential corresponding to the beam energy. It can be switched "on" and "off" by a fast high voltage switch (Behlke HTS-81-03-GSM Options DLC-ISO-HFS). The switch is equipped with water cooling and therefore a maximum toggle frequency of up to 100 kHz could be achieved over days of operation. During the "on"-period ions travel into the tube and during the "off"-period they travel out of the tube without seeing the fringe field at the entrance and exit of the tube. The ions which are not in

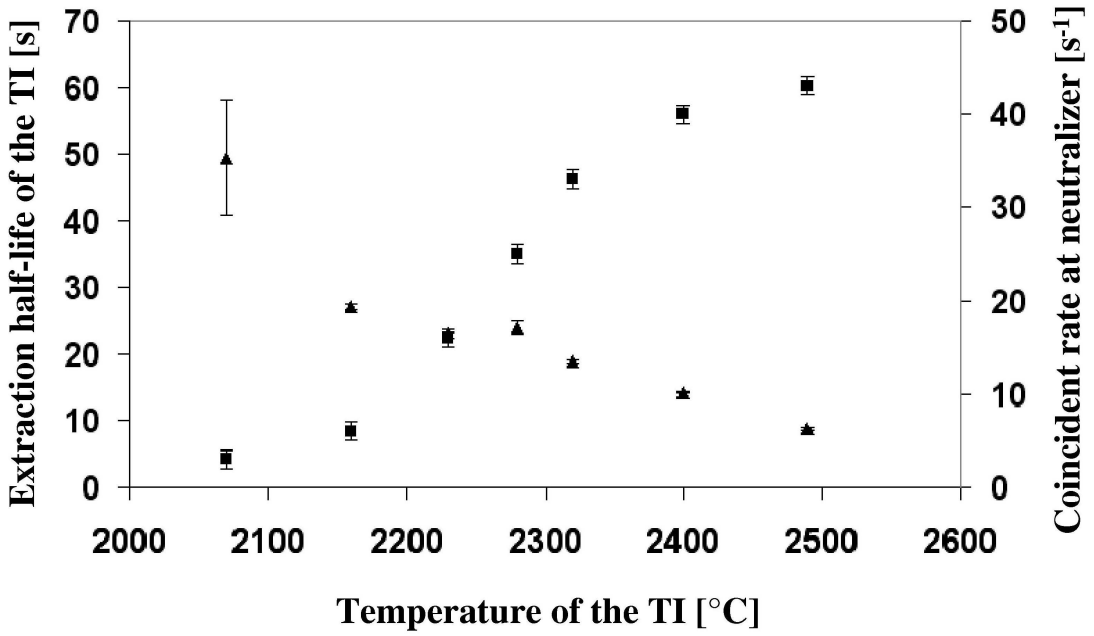

Fig. 4.10: Temperature dependence of the extraction half-life of the TI (▲) and rate of the ^{21}Na decay at the neutralizer in the trap chamber (■). The extraction half-life ($\mathcal{T}_{TI}$) drops at higher temperatures and the extraction yield increases.

phase are lost. In the optimal case the on-period of the tube allows to fill the tube completely. The duty cycle of the tube D is defined as the ratio of the "on"-period of the tube t to the full pulse period at the optimal condition τ

$$\begin{aligned} D &= \frac{t}{\tau}, \\ \tau &= \frac{2l}{c\sqrt{\frac{2E}{M}}} \end{aligned} \tag{4.7}$$

where l is the length of the drift tube, E is the ion energy and M is the ion mass. With the length of the tube l =100 cm and with $1/\tau$ =60 kHz a duty cycle of 45% is achieved for ^{21}Na isotopes at 2 keV energy.

In the LEBL we have an microchannel plate (MCP) detector to detect ions. It is equipped with a phosphorescence plate at its back to convert the current intensity into light which is observed by a commercial CCD camera. Different ions which are extracted from the TI are seen on the MCP detector by scanning the Wien-filter's electric field. A spectrum of the masses which was obtained this way, is shown in figure 4.11(a). Here the time of flight t_{TOF} is measured between the end of the drift tube and the MCP detector. The mass (M) of the ion is given

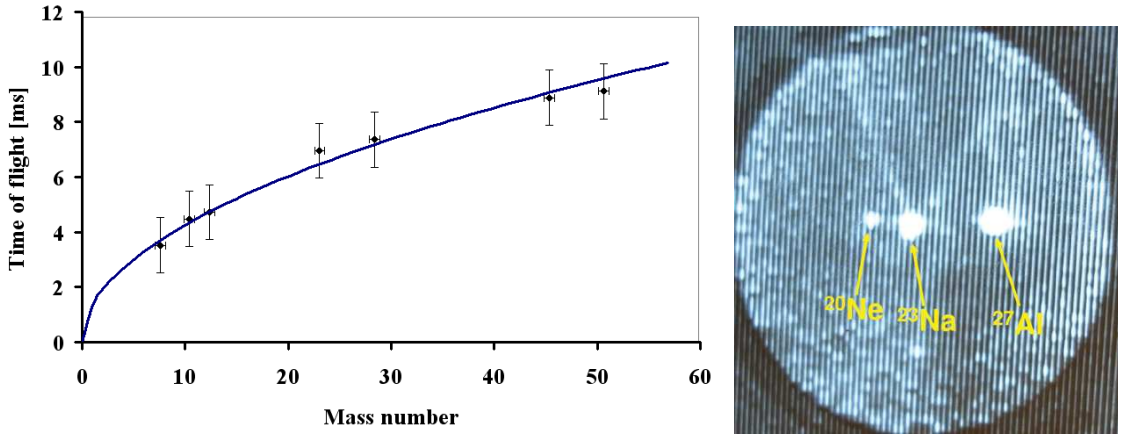

(a) (b)

Fig. 4.11: a) The TOF of different masses separated by the Wien-filter and observed at the MCP detector. The energy of extracted ions is 2.8 keV. b) Ne and Na spots on the MCP detector. Adding natural Ne gas in the TI produces a signal at mass A =20 as a reference. The full size of the MCP is 4 cm diameter.

by

$$M = \frac{2E}{d^2}\, t_{TOF}^2, \tag{4.8}$$

for an ion energy E and a distance of the ion travel d. For ions with 2.8 keV energy and for $d = 1$ m the mass number is:

$$A = 0.5356(\mu s)^{-2}\, t_{TOF}^2. \tag{4.9}$$

For calibration a small amount of natural Ne gas ($\sim 6\times10^{-6}$ mbar.l/s) was leaked into the TI to identify the mass A =20. Figure 4.11(b) shows the Ne isotopes close to mass A =23 from natural Na. The position resolution on the MCP allows mean resolution of 1 u in the region of Na isotopes.

4.2.3 Collector MOT

In the collector MOT cell we need to neutralize incoming ions and trap the radioactive atoms. The ions are stopped on a hot zirconium foil as a neutralizer. Due to the high temperature (1000-1200 ° C) neutral atoms diffuse out of the foil and enter the laser beams. The capture velocity of the collector MOT with 1 cm diameter laser beams and 100 mW laser light is about 25 m/s. The probability to capture atoms coming out of the hot neutralizer in to the MOT is less than 10^{-4}

Table 4.2: Summary of the neutralizer measurements. The signal is from the position modulated MOT at 30 Hz frequency. All the neutralizers are cold.

Neutralizer material	Zr	Ti	Nb	LiF	Stainless Steel
Lock-in signal [arb.]	1.3	0.3	2.5	0.4	0.2

(see Fig. 4.12). The efficiency of metal foils to release neutral atoms is related to their temperature. A higher temperature leads to faster effusion of the atoms. Therefore we need a compromise between the neutralization efficiency and the MOT capture efficiency.

Off-line measurements of different neutralizer foils were performed to find the most suitable neutralizer material for Na ions. An ion gun produces several nA Na ion current with a few keV energy on the hot neutralizer foil which is kept at ground potential. The foil of 5 mm width, 10 mm length and 20 μm thickness is spot welded to two stainless steel wires of 2 mm diameter, which are mounted on a UHV electric feedthrough. The foil can be resistively heated and 6 A of current produces a temperature of about 1200 K.

Neutralized atoms are trapped in the MOT which is monitored by a photomultiplier tube (PMT) using an optical imaging setup with a pinhole between two 50 mm focusing lenses to cut stray light. In order to improve the signal-to-noise ratio the MOT position was modulated by an oscillating magnetic dipole field superimposed on the traps static quadrupole field and orthogonal to the observation direction. Lock-in detection was employed for the fluorescence signal detection from the MOT cloud. A typical signal is shown in figure 4.13. The strength of the signal for different neutralizer materials is tabulated in table 4.2. The heating of the neutralizer causes a significant increase in the gas pressure in the cell which is affecting the MOT lifetime and therefore makes the interpretation of the results more difficult. From the cold neutralizer results one expects that Nb would be the best material for Na ion neutralization. In the long run Nb showed a significant loss of signal which is probably due to its surface quality. The Zr foil has a more stable and reproducible behavior. Crystalline LiF was suggested as possible neutralizer material due to its higher conductivity relative to other dielectric materials specially in grazing ion incidence [Mey97, Wir01, Wir03]. In our measurement we used a 9 mm diameter, 3 mm thick LiF crystal with an optical quality surface and normal ion impact. It shows a small neutralization

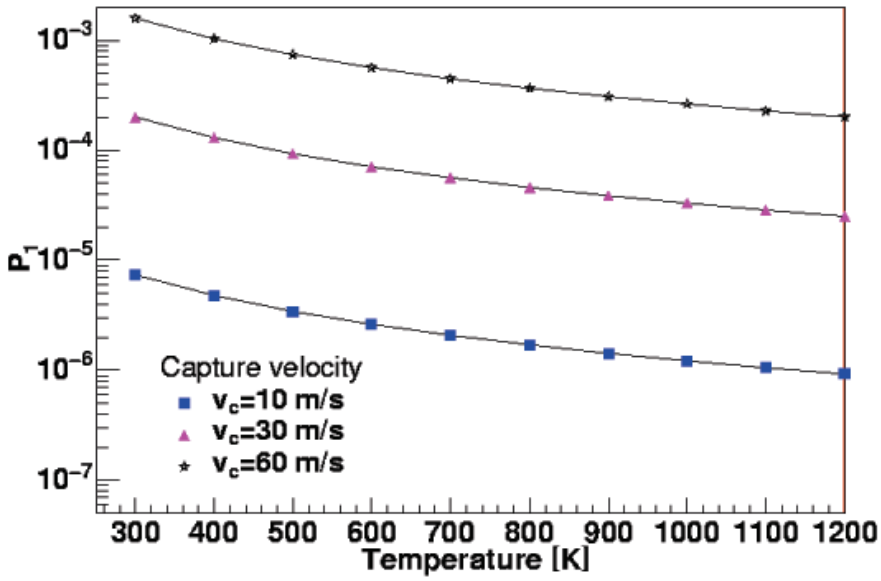

Fig. 4.12: Single pass capture probability P1 for neutral atoms in a MOT (see Eq. 3.7) as a function of temperature for a number of capture velocities v_c from a three dimensional thermal gas.

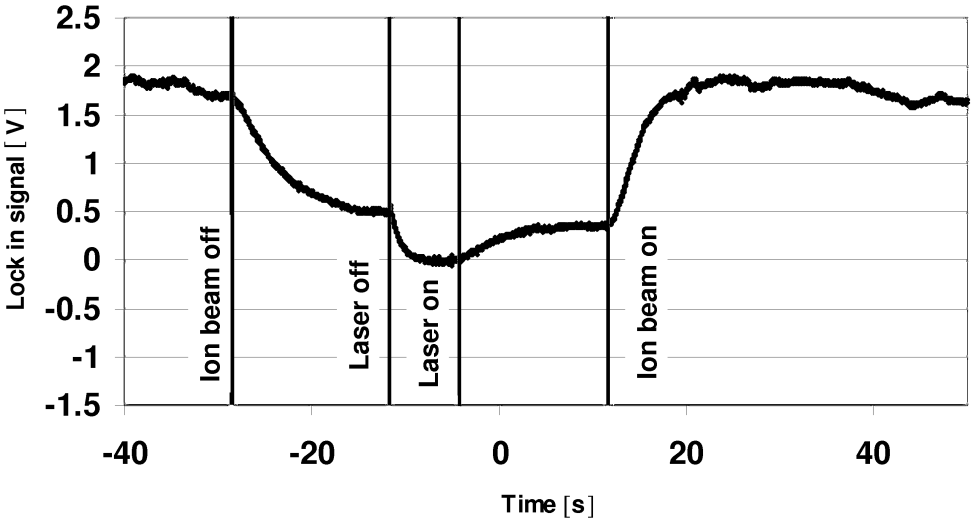

Fig. 4.13: Signal from a modulated MOT cloud. Atoms are captured after neutralization on a Zr foil of ^{23}Na beam from an ion source. The lock-in amplifier integration time of 10 s defines the decay and rise times of this signal. The signal demonstrates that a Na beam can be neutralized and the atoms can be captured in a MOT.

signal, but by far not as good as metal foils.

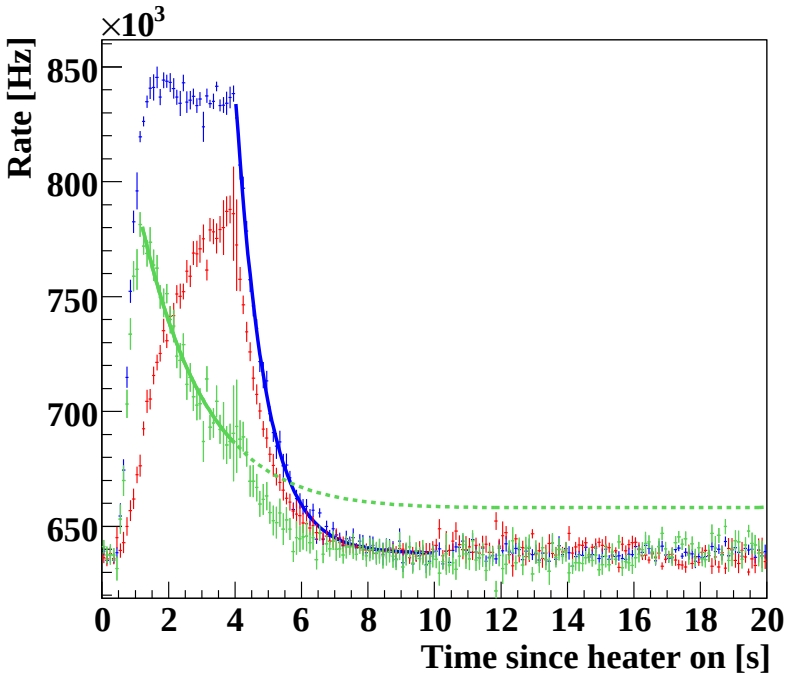

Fig. 4.14: The PMT signal from the collector MOT. It is loaded with neutralized ^{23}Na atoms from the TI (blue) and from the neutralizer bulk material (red). The neutralizer is heated within 4s of a 20 second period. The difference of the two signals shows the beam related signal part (green) which has an offset.

4.2.4 Trapping Efficiency

A measurement of the collector MOT trapping efficiency was conducted using a ^{23}Na ion beam extracted from the TI at 80 pA current. It hit the Zr neutralizer foil which was heated to about 1100 °C periodically for 4 s every 20s by switching a current through it. Figure 4.14 compares two data sets with and without ion beam. The photon detection has a fast rise after heating the neutralizer with ion beam being on in comparison with the ion beam off. The Na atoms from the beam stop close to the surface of the foil and can diffuse faster, if the foil is hot. The Na atoms from the bulk material itself need more time to diffuse out of the foil. Therefore subtracting the two signals gives the beam related signal, which has a fast rise-time and a slow decay-time. Using a fit and extrapolation gives a constant level of about 15×10^3 photon counts per second above the

background level. This means that keeping the neutralizer hot gives a visible beam related increase to the MOT signal. The difference of the number of the photon detection relative to the number of incoming ions gives a detection photon count rate of 2.5×10^{-5} per incoming ion after neutralization and trapping in the MOT. This number includes all efficiencies for neutralization, trapping and the photon detection chain efficiency. A MOT lifetime of 800 ms is measured by fitting the decay part of the spectrum. It is consistent with 4×10^{-8} mbar residual gas pressure in the MOT cell [Bjo88]. The same setup will be used to trap and detect ^{21}Na atoms.

4.3 β-decay Detection Setup

The β-decay precision measurements take place in a UHV chamber. A second MOT, the measurement MOT, is located in a reaction microscope [Ull97] and in the vicinity of a β-particle detector.

4.3.1 Detection Method

The detection system consists of a reaction microscope and a β-calorimeter. The MOT cloud is located at the center of a UHV chamber at 10^{-10} mbar residual gas pressure. The energy of the recoil-ion after a β-decay is small compared to the energy of the leptons, because the recoil-ion has much higher mass than the leptons. For the ^{21}Na decay the maximum energy of the recoil-ion (^{21}Ne) is about 230 eV (see Fig. 4.15) and the maximum energy of the positron is 2.5 MeV. One can collect and guide the ions using a sufficiently strong electric field and achieve thereby 4π detection. Recoil-Ion-Momentum Spectroscopy (RIMS) in combination with a MOT is an advanced method. It is employed at KVI e.g. to study charge exchange processes with recoil-ion energies of order eV [Tur01, Kno05].

The MOT-RIMS technique is applied to the β-decay measurements by collecting radioactive atoms in a small localized trapped cloud (see Fig. 4.16). An electric field produced by a set of electrodes projects the recoil ions coming from the MOT cloud onto a MCP detector. The ion travels along a ballistic trajectory and hits the surface of the detector. An amplified pulse of electrons is produced at the output of the MCP at the position of the hit. This electron pulse can be collected on a position sensitive anode to resolve the position of the incoming ion. A time-of-flight measurement for the recoil-ion is started by observing a hit

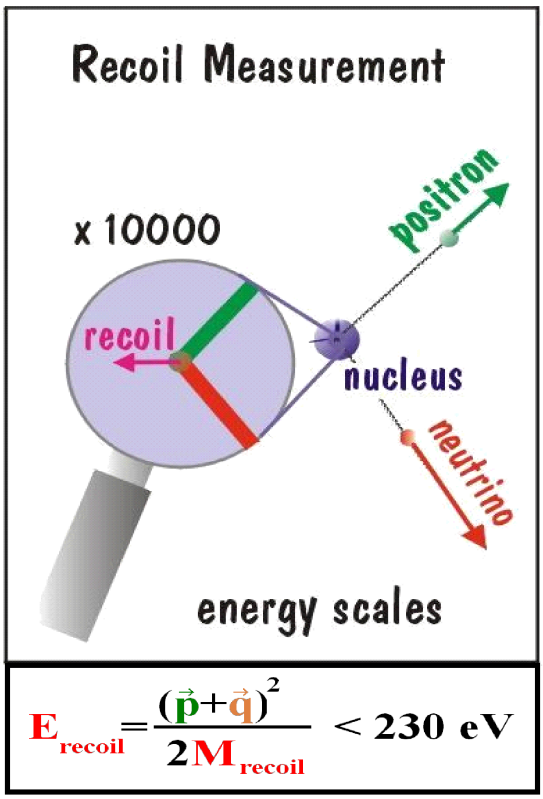

Fig. 4.15: Energy of the recoil-ion in the ^{21}Na decay.

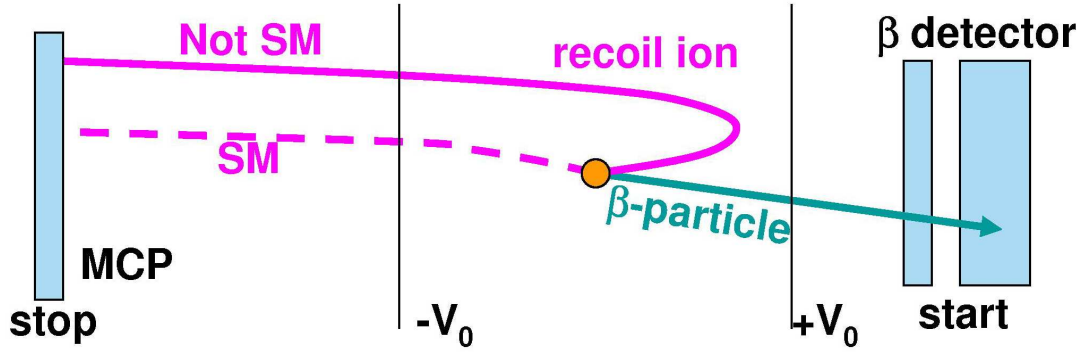

Fig. 4.16: Sketch of RIMS of a β-decay. The dashed line indicates a typical trajectory of the recoiling ion for a SM decay and the solid line gives a non-SM decay for a Fermi β-decay.

from the simultaneously released β-particle on the β-detector and it is stopped by the hit on the MCP. The time of flight and the position of the recoil-ion on the MCP provide complete kinematic information about the momentum of the recoil-ion after the β-decay.

In contrast to the full coverage for the recoil-ion detection, the β-detector has a limited acceptance because of its geometrical solid angle. There are three positions foreseen in the setup to mount a β-detector assembly. One in the direction of the axis of the reaction microscope and two orthogonal to it. Each detector covers about 9% of the full solid angle. A position sensitive β-detector allows to restrict the momentum of the β-electron.

A combination of MOT-RIMS and β-detectors have been employed successfully in precision experiments for limited β-decay studies [Tur00, Sci04, Gor05]. The detection system described here has the advantage of position sensitivity on both reaction microscope and β-detector. This is essential for detailed kinematic studies of β-decay.

4.3.2 MOT in the Detection Chamber

The detection chamber containing the detection MOT is a 200CF double cross vacuum chamber with 4 additional 63CF ports for lasers and 4 additional 40CF ports for monitoring (see Fig. 4.8, 4.17 and 4.18). The inner free diameter of this chamber (30 cm) is one order of magnitude larger as compared to the collector MOT (2.5 cm). The magnetic field coils of 290 mm inner diameter for the MOT are mounted outside of the vacuum chamber and operated in anti-Helmholtz mode. They have 16 windings each and they are separated by 28 cm. Due to the large distance between the coils a current of 300 A is needed to produce a magnetic field gradient of 20 Gauss/cm. The coils are made of copper tubing to allow for water cooling.

Six laser beams overlap in the MOT region of 2 mm diameter in the geometrical center of the chamber which is also the center of the detection system. A magnetic field map near the center of the chamber was recorded using a Hall probe (see Fig. 4.19). All the coordinates of the field vector were measured for 150 A current in the coils and for the background. The effect of the earth magnetic field and the distortion caused by the laser table under the detection chamber can be seen (see Fig. 4.20). A shift in the position of the zero field point relative to the center of the chamber of 2 cm is observed. Figure 4.21 shows the calculated magnetic field of the coils and its gradient for 342 A. A set of three

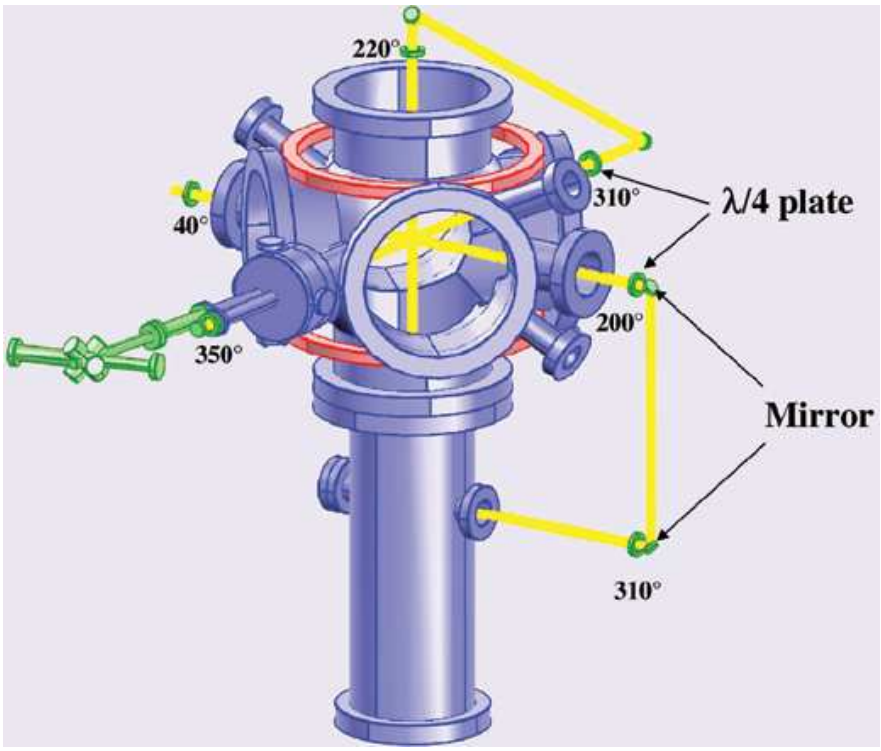

Fig. 4.17: Layout of the MOT setup in the detection chamber. The actual angle of the $\lambda/4$ plates with respect to the optical axis is given.

circular correction coil pairs are mounted on the 200CF flanges in order to correct the field distortions. These coils allow to shift the zero field region by a few centimeters which is sufficient to assure overlap of the zero magnetic field region with the laser beams.

The required 6 laser beams are provided by sending a single beam with appropriate mirrors and retardation birefringent optics through the chamber. It is circulated through the chamber such that it travels along all three orthogonal axes and it is finally reflected back onto itself (see Fig. 4.17). The optical windows are antireflection coated to minimize the light losses at below 0.1% per surface. Natural Na was trapped in this chamber with 50 mW of laser power and 300 A current in the main coils (see Fig. 4.22).

The TRIμP facility, in particular the collector MOT and the MOT in the detection chamber work completely satisfactory to fulfill the needs of a precision β-decay experiment on ^{21}Na.

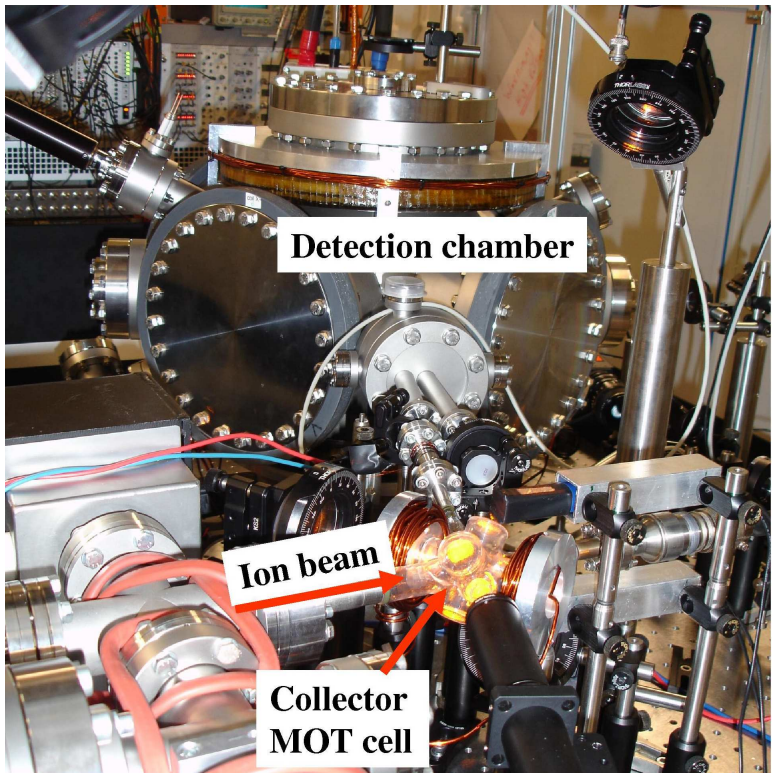

Fig. 4.18: Atomic trap and detection setup.

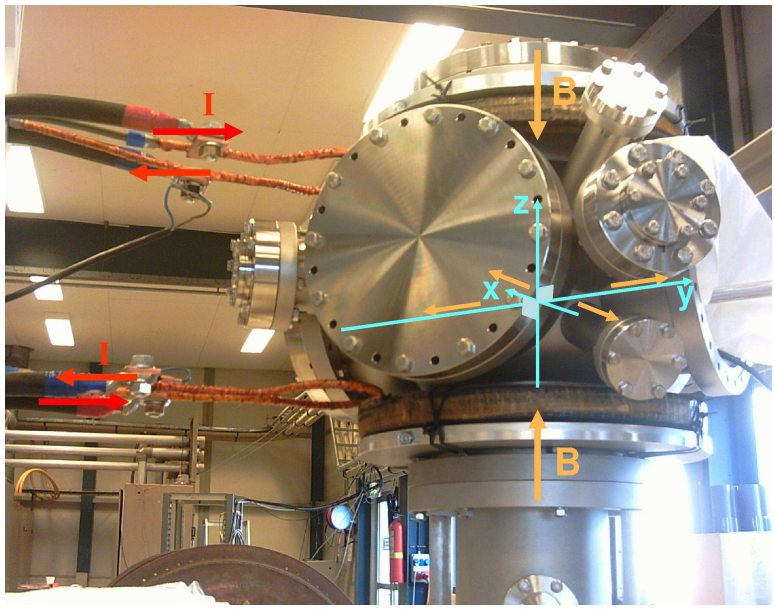

Fig. 4.19: Magnetic field measurement setup. The direction of the current I in the coils and the magnetic field B are indicated.

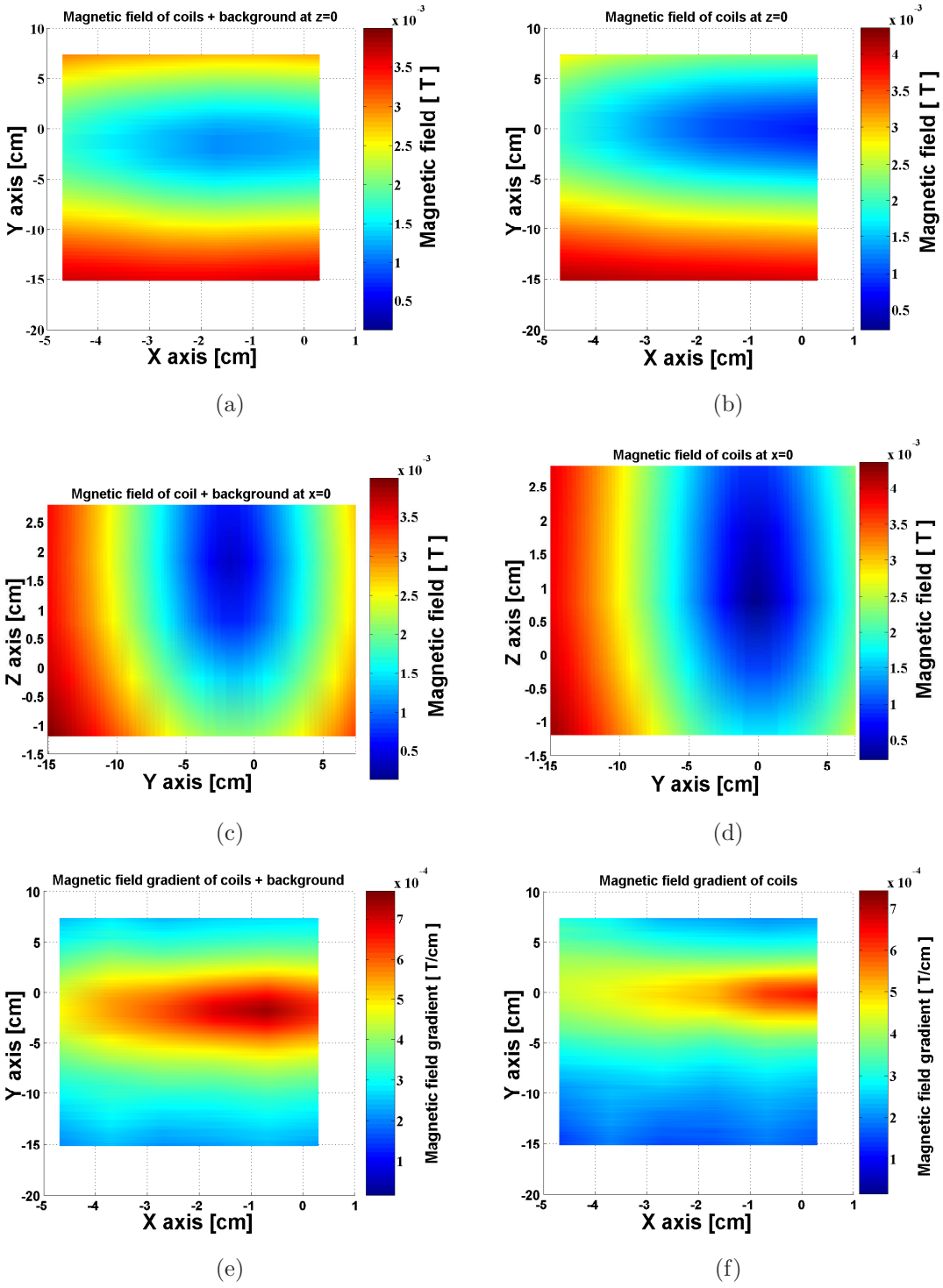

Fig. 4.20: Measured magnetic field map with background (a) and (c) and with subtracted background (b) and (d). Measured magnetic field gradient with background (e) and after subtracting background (f).

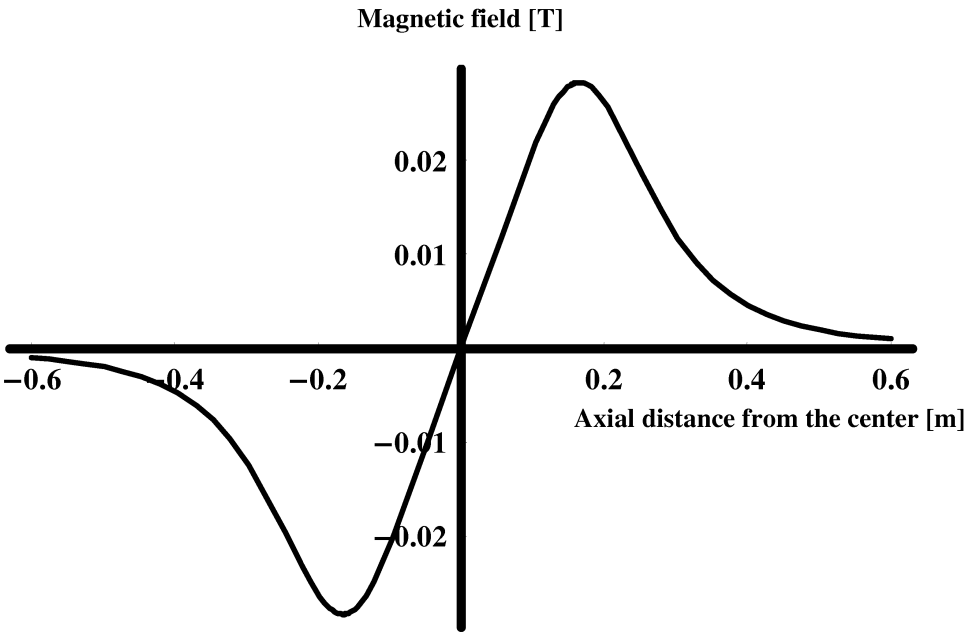

(a)

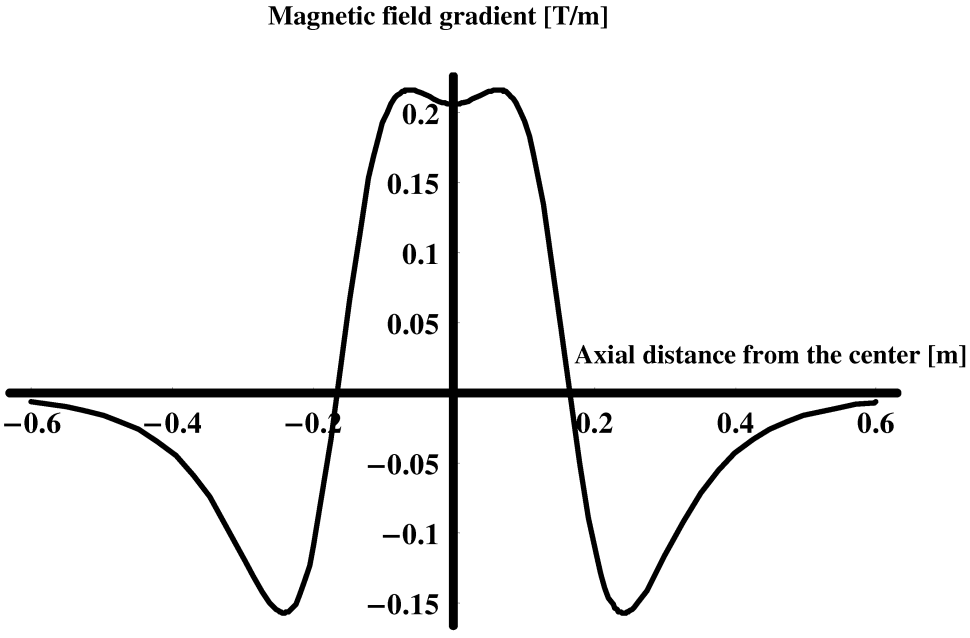

(b)

Fig. 4.21: Magnetic field (a) and its gradient (b) in the detection chamber for 342 A current.

Fig. 4.22: Fluorescence from a MOT cloud containing ^{23}Na in the detection chamber. The diameter of the MOT cloud is smaller than 1 mm.

4.4 Conclusion

The TRIμP facility has now reached a state such that it can be used for the foreseen precision experiments. In particular,

a) it has capability to produce clean and intens radioactive secondary beams with its dual magnetic separator, e.g. up to 3×10^6 ^{21}Na/s for 100 W primary beam and 1 bar gas target pressure with better than 99.5% purity.

b) it provides the opportunity to use high intensity primary beam and pressured gas target to increase the up to now recorded number of events in future precision experiments. A primary beam of up to 1 kW ^{20}Ne at 23 MeV/nucleon and gas target pressure of 10 bar can be expected from linear extrapolation of measured data at up to 5 bar pressure and independently 300 W primary beam.

c) it has operational apparatuses for slowing and cooling radioactive ion beams, namely a thermal ionizer with 50% efficiency for ^{21}Na and a RFQ cooler with 56% transmission.

d) there is an atomic MOT setup which is particularly suited for Na isotopes.